Search for Fusion from Energy Focusing Phenomena in Ferroelectric Crystals

B. Naranjo and S. Putterman
Physics Department, University of California, Los Angeles, CA 90095

1 February 2002

Abstract

This research is motivated by the observation that ferroelectric crystals spontaneously emit electrons and ions with energies approaching or exceeding 100 keV. These emissions can be generated simply by heating or cooling the crystals. Furthermore, these energies are high enough to cause fusion between deuterium nuclei. Based upon these observations we propose to search for fusion from deuterated ferroelectric crystals.

Introduction

Nuclear fusion, along with other clean burning renewable resources, is a promising long term alternative to fossil fuels. For example, deuterium nuclei, abundant in seawater (30 g/m^3), undergo the fusion reactions

$$^2\mathrm{D} + {}^2\mathrm{D} \rightarrow {}^3\mathrm{He}\,(0.82\,\mathrm{Mev}) + \mathrm{n}\,(2.45\,\mathrm{MeV}) \quad \text{and} \tag{1}$$

$$^2\mathrm{D} + {}^2\mathrm{D} \rightarrow {}^3\mathrm{T}\,(1.01\,\mathrm{Mev}) + \mathrm{p}\,(3.03\,\mathrm{MeV}), \tag{2}$$

whose environmental hazards, including neutron induced activation and tritium production, can be confined to the reactor via careful design. Though progress in fusion technology continues steadily with magnetic confinement[1] and inertial confinement[2], we should also investigate novel fusion schemes, such as Coulomb explosion of deuterium clusters[3], for their insight into basic fusion processes and potential technological applications. In this spirit, we propose using the large ($\sim 10^8$ V/cm) transient fields observed in ferroelectrics to drive a compact pulsed low-yield fusion device. Our goal will be to demonstrate technical feasibility.

Current Work at UCLA

We have pursued an interest in natural energy focusing processes. For example, sonoluminescence (SL), the transduction of sound into light, pushes fluid mechanics beyond its limit. An initial state with long wavelength and low Mach

number, as is realized for a gas bubble driven by an audible sound field, spontaneously focuses energy densities 12 orders of magnitude[4], generating supersonic motion, a different phase of matter, and picosecond flashes of broad-band UV light.

Our main insight into SL is that the spectrum of light emitted by a single bubble of gas, pulsating synchronously with a typical 40 kHz sound field, fits a blackbody curve. The blackbody temperature and radius of emission range from 20000 K and 0.1 μm for a helium bubble to 6000 K and 0.25 μm for a hydrogen bubble[5].

At substantially higher frequencies, such as 10 MHz, we have observed SL from a cloud of bubbles formed at the focus of a spherical transducer. Our measurements indicate that these bubbles are less than 10 nm in radius[6]. These spectra do not fit a blackbody but instead fit bremsstrahlung emission from a transparent plasma whose temperature's lower bound is 10^5 K.

The strength of the bubble collapse is so strong that pressure jumps approaching 1 Mbar are observed[7].

We have found that light emission increases with lower ambient fluid temperature. For example, a bubble at 0° can be 100 times brighter than a bubble of the same size at 30°[8].

The intensity of SL from helium and xenon bubbles are similar. In view of the very different ionization potentials this could not happen in a weakly ionized plasma. If SL originates in a plasma, then this plasma must be strongly coupled[9].

Another energy focusing phenomenon we have studied is friction. We observed that mercury sliding relative to glass ($\sim$1 mm/s) repetitively generates picosecond 25 eV electron bursts[10], and then showed that this effect plays a role in everyday stick-slip friction[11].

We now apply our perspective to the possibility that ferroelectric emission is another dramatic energy focusing process.

Ferroelectrics

Materials having a spontaneous polarization P_s in the absence of an external field are called pyroelectric. Ferroelectrics are pyroelectric materials whose polarization can be reversed by applying an external field of strength $E > E_c$.

For most ferroelectrics, P_s decreases with temperature from a maximum at absolute zero and then vanishes at the Curie point T_C. $P_s(T)$ for $LiTaO_3$ is shown in figure 1.

The basic concept of ferroelectric emission is illustrated in figure 2. We connect a grounded electrode to one of the sample's polar faces and place a grounded mesh near the other face. A typical experiment might use sample width $a = 1$ mm and gap width $d = 10\,\mu$m. While in the initial equilibrium state, where free charge screens the polarization charge, we alter the spontaneous polarization by ΔP_s. This can be done by varying the temperature ($\Delta P_s = \gamma \Delta T$), applying a reversing field ($\Delta P_s = 2P_s(T)$), or the piezoelectric effect. Changing the

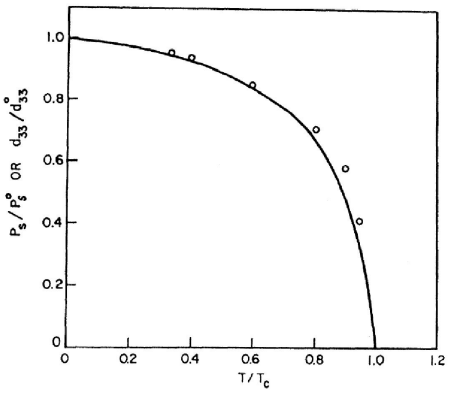

Figure 1: $P_s(T)$ for $LiTaO_3$[12]. $T_C = 618$ K, $P_s(0) = 53$ μC/cm^2, and $P_s(300) = 50$ μC/cm^2

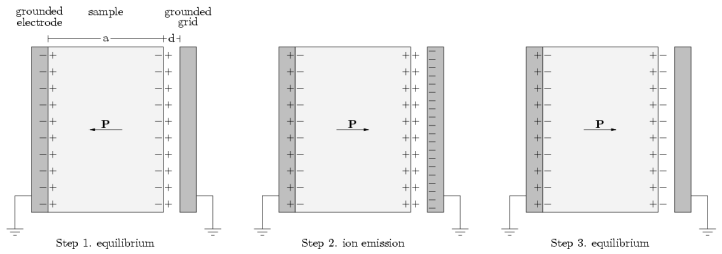

Figure 2: Reversing the spontaneous polarization creates a large electric field in the gap.

polarization redistributes the polarization surface charge. The attached electrode acts quickly to screen out the difference, but the other face isn't screened immediately since the the sample has low bulk conductivity ($\tau = \epsilon\epsilon_0/\sigma \sim 10^6$ s for $LiNbO_3$). In fact, the screening current is due to emission or absorption of charge carriers at the surface[13]. We estimate the field in the gap (for $a \gg d$) as

$$E_a = \frac{\Delta P_s}{\epsilon_0}. \tag{3}$$

For example, reversing $LiTaO_3$'s polarization at room temperature gives a field strength of $E_a \sim 10^9$ V/cm. Note that above 10^8 V/cm, deuterium molecules in the vicinity of the positively charged surface are easily field ionized[14].

Large ion and electron energies have been reported. For example, 133 keV ions and 170 keV electrons were emitted from a $LiNbO_3$ crystal by thermally cycling between room temperature and 115°C in a rarefied atmosphere of dry nitrogen[15][16].

Ferroelectric cathodes capable of intense (> 10 A/cm^2) and rapid (> 2 MHz)

pulses (50-200 ns long) have been developed at CERN for use in electron guns[17].

Proposed Experiment

Our quest for a new source of fusion will be carried out in a vacuum environment with various ferroelectrics. Heater wire and a recirculating chiller will be used for temperature control. The general aim is to accelerate deuterons onto a solid deuterated target, noting that the neutron yield (approximately one half the fusion yield) for 100 keV deuterons accelerated into a D_3PO_4 target is $8.7 \times 10^4/\mu$C[18].

Among other experiments, we will try the following:

- deuterated triglycine sulfate (DTGS)
- lithium niobate ($LiNbO_3$) in a low pressure deuterium gas environment
- lithium tantalate ($LiTaO_3$) in a low pressure deuterium gas environment
- $LiNbO_3$ placed back to back with DTGS

Neutron Detection

The heart of a search for new routes to fusion is a neutron detector capable of time correlated single neutron counting. Roughly half of DD fusion events occur by neutron emission (eq. 1) and half by proton emission (eq. 2). We will ascertain the presence of DD fusion reactions by looking for the outgoing 2.45 MeV neutron. Figures 3 and 4 show a detector which has already been constructed at UCLA as part of a DARPA funded project to search for the limits of energy focusing in SL. The detector comprises twelve independent channels, each consisting of a glass cell containing organic liquid scintillator coupled to a 5" PMT. One of the PMT's anode outputs is connected to a 1 GS/s 8-bit digitizer and the other output is discriminated and connected to a custom trigger module. The trigger module performs various functions, and, being driven by an FPGA, is easily reprogrammed to suit the application. We have a total of 14 digitizer channels which are trigger and clock synchronized to obtain a complete record of each event, facilitating various tagging analyses. For example, if there is fusion, we will be able correlate it with prompt x-ray emission, and even measure neutron energy via time-of-flight. The digitizers are on a PCI bus, and so have a fast sustained readout approaching 110 MB/s, allowing for low dead time. Discrimination between neutrons and gammas is accomplished by analyzing the scintillator's pulse shapes. One compares the light signal in the tail of a track to the light signal in the peak. For neutrons, the light signal in the tail is a greater percentage of the total light, a property of organic liquid scintillator. Figure 5 shows the neutron and gamma branches for a ^{252}Cf source. The 2.45 MeV neutrons that we seek will lie on the upper branch near the diagonal line that intersects the x-axis at 475. The separation between n and γ is obviously good.

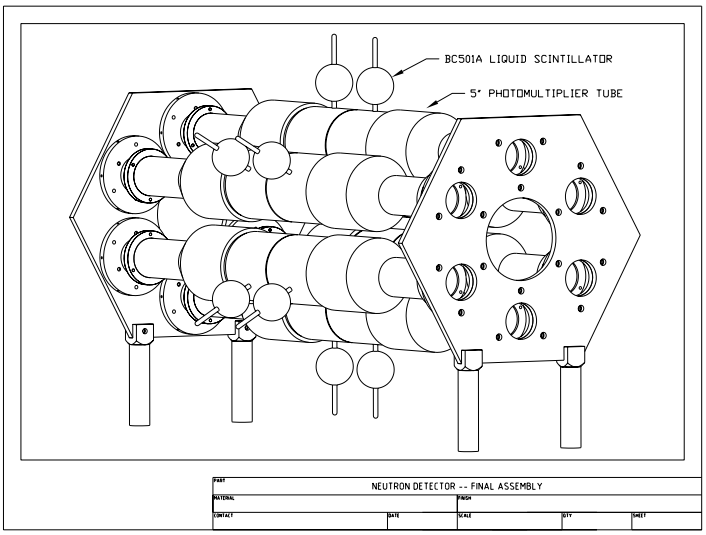

Figure 3: CAD drawing of neutron detector, where the outer skin has been removed for clarity. The central bore's diameter is 6.125".

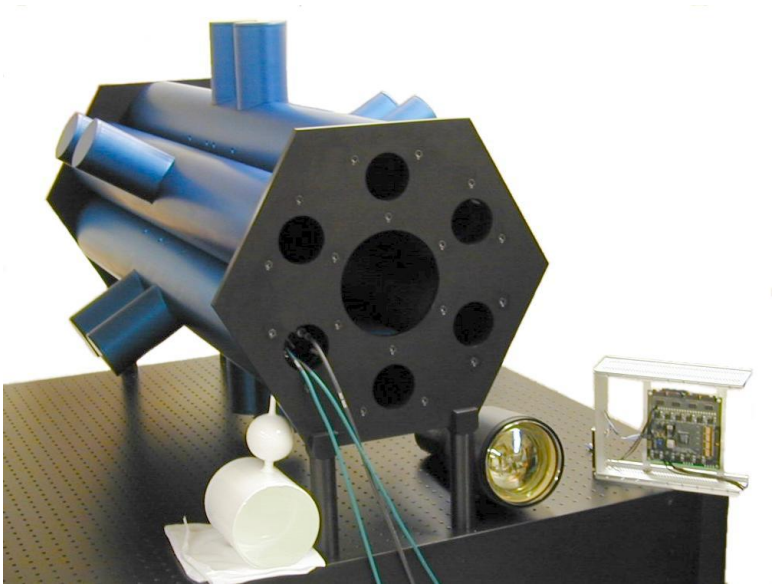

Figure 4: Assembled neutron detector. Note the liquid scintillator, photomultiplier, and custom electronics module.

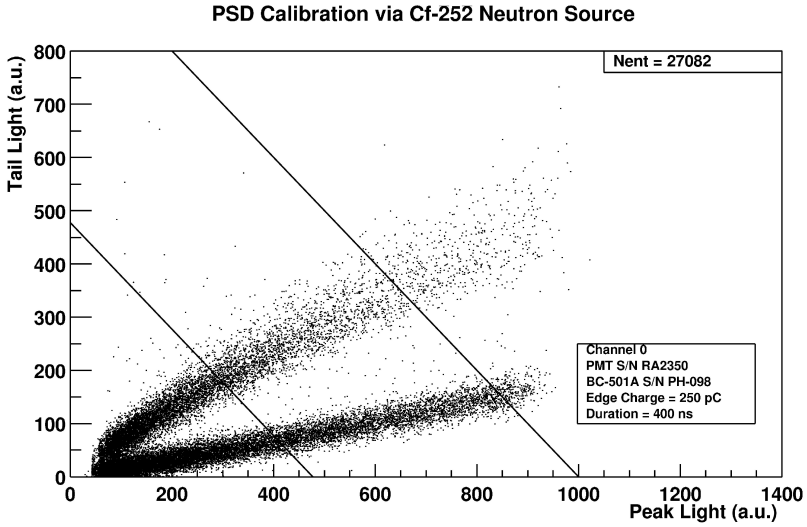

Figure 5: Neutron/gamma pulse shape discrimination obtained with our neutron detector. The upper branch is the neutron branch.

Funding Schedule

It will take about three months to obtain the crystals, build an appropriate holder and heater, and verify the existence of electron emission in the 100 keV range. These experiments will be then coupled to our neutron detector. We will then spend the next 4 months searching for fusion from deuterated crystals. If a positive signal is obtained, we will immediately apply for extramural funding.

References

[1] R. Maingi *et al.*, Phys. Rev. Lett. **88**, 35003 (2002).

[2] R. Kodama *et al.*, Nature **412**, 798 (2001).

[3] J. Zweiback *et al.*, Phys. Rev. Lett. **84**, 2634 (2000).

[4] S. Putterman and K. Weninger, Annu. Rev. Fluid Mech. **32**, 445 (2000).

[5] G. Vazquez, C. Camara, S. Putterman, and K. Weninger, Optics Lett. **26**, 575 (1998).

[6] K. Weninger, C. Camara, and S. Putterman, Phys. Rev. E **63**, 16310 (2001).

[7] K. Weninger, P. Evans, and S. Putterman, Phys. Rev. E **61**, 1020 (2000).

[8] G. Vazquez and S. Putterman, Phys. Rev. Lett. **85**, 3037 (2000).

[9] S. Putterman, P. Evans, G. Vazquez, and K. Weninger, Nature **409**, 782 (2001).

[10] R. Budakian, K. Weninger, R. Hiller, and S. Putterman, Nature **391**, 266 (1998).

[11] R. Budakian and S. Putterman, Phys. Rev. Lett. **85**, 1000 (2000).

[12] A. M. Glass, Phys. Rev. **172**, 564 (1968).

[13] G. Rosenman, D. Shur, Y. E. Krasik, and A. Dunaevsky, J. Appl. Phys. **88**, 6109 (2000).

[14] H. D. Beckey, in *Principles of Field Ionization and Field Desorption Mass Spectrometry in Analytical Chemistry*, edited by R. Belchev and H. Frieser (Pergamon, New York, 1977).

[15] J. D. Brownridge and S. M. Shafroth, Bull. Am. Phys. Soc. **46**, 106 (2001).

[16] J. D. Brownridge and S. Raboy, J. Appl. Phys. **86**, 640 (1999).

[17] H. Riege, I. Boscolo, J. Handerek, and U. Herleb, J. Appl. Phys. **84**, 1602 (1998).

[18] R. Roberts, Phys. Rev. **51**, 810 (1937).